

2005

Extreme Rainfall in Texas: Patterns and Predictability

John W. Nielsen-Gammon
Texas A&M University

Fuqing Zhang
Texas A&M University

Andrew M. Odins
Texas A&M University

Boksoon Myoung
Chapman University, bmyoung@chapman.edu

Follow this and additional works at: https://digitalcommons.chapman.edu/scs_articles



Part of the [Atmospheric Sciences Commons](#), [Meteorology Commons](#), and the [Other Oceanography and Atmospheric Sciences and Meteorology Commons](#)

Recommended Citation

Nielsen-Gammon, J. W., F. Zhang, A. M. Odins, and B. Myoung, 2005: Extreme rainfall in Texas: Patterns and predictability. *Phys. Geog.*, 26, 340-364. DOI: 10.2747/0272-3646.26.5.340

This Article is brought to you for free and open access by the Science and Technology Faculty Articles and Research at Chapman University Digital Commons. It has been accepted for inclusion in Mathematics, Physics, and Computer Science Faculty Articles and Research by an authorized administrator of Chapman University Digital Commons. For more information, please contact laughtin@chapman.edu.

Extreme Rainfall in Texas: Patterns and Predictability

Comments

This is an Accepted Manuscript of an article published in *Physical Geography*, volume 26, in 2005, available online at DOI: [10.2747/0272-3646.26.5.340](https://doi.org/10.2747/0272-3646.26.5.340)

Copyright

Taylor & Francis

EXTREME RAINFALL IN TEXAS: PATTERNS AND PREDICTABILITY

John W. Nielsen-Gammon, Fuqing Zhang, Andrew M. Odins, and Boksoon Myoung

Cooperative Institute for Applied Meteorological Studies

Department of Atmospheric Sciences

Texas A&M University

College Station, Texas 77843-3150

Submitted to *Physical Geography* Feb. 20, 2004

Revised June 10, 2004

Abstract: Extreme rainfall, with storm total precipitation exceeding 500 mm, occurs several times per decade in Texas. Through a compositing analysis, the large-scale weather patterns associated with extreme rainfall events involve a northward deflection of the tropical trade winds into Texas, with deep southerly winds extending into the middle troposphere. One such event, the July 2002 South-Central Texas flood, is examined in detail. This particular event was associated with a stationary upper-level trough over central Texas and northern Mexico, which established a steady influx of tropical moisture from the south. While the onset of the event was triggered by destabilization caused by an upper-level vortex moving over the northeast Mexican coast, a succession of upper-level processes allowed the event to become stationary over south-central Texas and produced heavy rain for several days. While the large-scale signatures of such extreme rain events evolve slowly, the many interacting processes at smaller scales make numerical forecasts highly sensitive to details of the simulations. [flooding, rainfall, Texas]

INTRODUCTION

Many Texas rainfall events approach world records in rainfall intensity (Patton and Baker, 1977; Asquith 1998), and Texas is susceptible to greater extremes of precipitation than is any other part of the United States (Hirschboeck, 1987; Konrad 2001). While all parts of the state are subject to flooding, the steep drainages and shallow soils of the Texas Hill Country make that area especially vulnerable to large discharges (Patton and Baker, 1977; Smith et al. 2000). The South-Central Texas Flood of 2002, while an extreme event by many measures, is merely a recent example of a catastrophic Texas rainfall event, although moderate to extreme rainfall events may be increasing in frequency (Kunkel et al. 1999).

Surveys of the meteorological characteristics of flood-producing rainfall events, both nationally (Maddox et al., 1979) and within Texas (Grice and Maddox, 1983), have focused on non-tropical rainfall events. Those recent extreme Texas events that have been studied in detail, such as 1-4 August 1978 (Caracena and Fritsch, 1983), 17-21 September 1979 (Bosart, 1984), 16-19 September 1984 (Bosart et al., 1992), 16-19 October 1994 (Petroski, 2000), and 17-19 October 1998 (Scott, 2001), are notable for their superficial dissimilarity: some occurred in association with tropical cyclogenesis, others with tropical storm dissipation, and still others with no tropical cyclone whatsoever. Triggering and focusing mechanisms may have included coastal fronts, synoptic-scale fronts, topography, or merely large-scale ascent.

Absent a single pattern to use to rely on for recognizing an upcoming extreme rainfall event, forecasters must apply their basic knowledge of the intrinsic causes of heavy rain. Doswell et al. (1996) propose an “ingredients-based methodology”. Using the fact that extreme rainfall totals require a combination of high rain rates and long duration, they suggest that forecasters focus their efforts on predicting the necessary ingredients of ample moisture, ascent, high precipitation efficiency, slow storm motion, and storm extent along the axis of motion. The necessary amounts of each ingredient are left unspecified and are situation-specific (Shultz et al., 2002).

Help in forecasting extreme events might be expected to come from numerical weather prediction models, but models have more difficulty forecasting precipitation than any other important atmospheric variable, and the difficulty is particularly acute for warm-season, weakly-forced convective precipitation (Stensrud et al., 1994; Olson et al., 1995; Wang and Seaman, 1997). Dramatic increases in model resolution hold promise (e.g., Nicolini et al. 1993), but precipitation forecast skill appears to get systematically worse as the scale of verification decreases (Gallus, 2002; Colle et al., 2003).

Part of the problem with warm-season convective rainfall is that the evolution of the event may depend critically on the location of the initial outbreak of precipitation. Feedbacks on the rainfall distribution arise from latent heat release, compensating subsidence, and the development of a low-level pool of cold air. Forecasting the specific locations of extreme rainfall maxima may be intrinsically difficult or impossible, even with improved future technology.

The purpose of this paper is to explore the meteorological causes and predictability of the South-Central Texas Flood. A composite analysis identifies the large-scale weather patterns associated with extreme rain in Texas. The 2002 event is compared to these composite patterns, to see if the weather patterns during that time were recognizable as being associated with the potential for extreme rainfall. The detailed evolution of the weather patterns associated with this specific event is then analyzed. A set of numerical simulations is then described to investigate the ability of numerical models to reliably predict the amount and location of heavy rainfall during this event. As the scales of interest become finer, the predictability of the event becomes smaller.

COMPOSITE PATTERNS

Data and Methods

The data for the composite analysis is the NCEP/NCAR Reanalysis data (Kalnay et al., 1996), and the compositing was performed using tools available on the NOAA-CIRES Climate

Diagnostics Center, Boulder, Colorado web site at <http://www.cdc.noaa.gov/>. The reanalysis data, a set of six-hourly three-dimensional gridded analyses, extends from 1948 to the present.

For the purposes of this study, an extreme rainfall event is defined as an event which produced point total precipitation of at least 500 mm over at most seven days. A total of 18 such storms since 1948 are identified from the compilation of notable and extreme storms in Texas by Lanning-Rush et al. (1998). To this list we add two recent events from 1998 and 2001. The 2002 event also qualifies: the National Weather Service reported that 857 mm of rain fell at Helotes, Bexar County, over seven days, and radar-estimated rainfall exceeded 1000 mm in Kerr County. The events are listed in Table 1.

To focus on events taking place during the relatively stationary climatological weather patterns of summer and early fall, we exclude from compositing the events of 22-25 April, 1956, and 11-12 November, 1985. In order that it may be compared independently with the composites, the 2002 event is also excluded.

The remaining 18 events span 5 months. Because climatological flow patterns change substantially over the 5-month period, three subgroups are defined. The EARLY subgroup consists of the 5 events associated with tropical cyclones that took place in June, July, and early August. The LATE subgroup consists of the 4 events associated with tropical cyclones in September. The NONTROP subgroup consists of the 9 events not associated with tropical cyclones. All but one of the NONTROP events took place in September and October.

Composites are performed with respect to 0000 UTC on the date corresponding to the onset of the heaviest precipitation (Table 1). Composites of the weather patterns exactly one year after each event provide a reference depiction of typical conditions during the times of year in which

the events occurred. Two-year composites were also constructed; they are similar to the one-year composites and are not shown here.

The statistical significance of key aspects of the composites are estimated by randomly drawing 1000 samples of (5, 4, 8) members from (June 1 through August 8, September, September and October) for comparison with the (EARLY, LATE, NONTROP) composites. For the purposes of this comparison, the NONTROP event that took place in June 1948 is excluded from the NONTROP composite. The samples are extracted from the NCEP/NCAR reanalysis during the period 1948-2003.

Results

The EARLY composite of 850 hPa winds (Fig. 1a) features strong trade winds extending northwest across Yucatan into the Gulf of Mexico, feeding large amounts of moisture from the tropical Atlantic and Caribbean Sea across the coasts of Texas and Louisiana. The reference composite (Fig. 1b) shows that wind from the Gulf of Mexico or Caribbean is a common phenomenon that time of year. Near Texas, the most prominent feature in the one-year composite is a wind maximum in western Oklahoma. This Plains low-level jet (Igau and Nielsen-Gammon 1998) is a common feature in late spring and early summer and further intensifies at night. The critical difference between the EARLY composite and typical conditions appears to be the relative magnitudes of the 850 hPa wind over the Gulf of Mexico and over the southern Plains. In the EARLY composite, the wind speed decreases from the Gulf to the Plains, implying low-level convergence and deepening low-level moisture. During typical conditions,

the wind is much stronger over the Plains, implying low-level divergence over Texas and therefore downward motion and shallower moisture.

The presence of tropical cyclones in all members of the LATE composite (Fig. 2a) causes the cyclonic curvature of the composite wind from southeasterly over the Gulf to easterly over central Texas. Despite the different wind direction over Texas, the LATE composite shares with the EARLY composite a continuous stream of air feeding into Texas from the tropical Atlantic and the Caribbean Sea. The convergence over Texas is not strong, but upward motion is implied by the orientation of the winds blowing directly from low surface elevations to higher terrain. In the reference composite (Fig. 2b), winds are weaker and less upslope, and a strong connection to the Caribbean is absent.

The NONTROP composite (Fig. 3a), like the other two, features strong winds entering Texas, much stronger than in the reference composite (Fig. 3b). The wind is curved anticyclonically, causing more upstream trajectories to originate near Florida and the Bahamas rather than the Caribbean. The deceleration over eastern Texas, combined with a lack of diffluence, implies convergence and upward motion.

In all three cases, the most important aspect of the low-level wind pattern appears to be the strong flow of moisture directly into Texas from distant upstream tropical or subtropical locations. To test the significance of this feature, the average vector wind along 90W spanning the strong composite winds is computed and compared to 1000 random samples. We hypothesize that heavy rain events correspond to unusually strong winds directed toward Texas along this longitude. We choose 90W rather than a location closer to the Texas coast to capture the transport from the Caribbean or the Bahamas.

The results are shown in Table 2. All three composites are found to possess significantly stronger wind speeds at a greater than 95% confidence level. In addition, a wind direction favoring direct transport toward Texas occurs in less than 1% of the random samples for the EARLY cases and less than 4% for the NONTROP cases.

Precursor signatures are sought by examining the composites two days prior to the events (Fig. 4). The precursor EARLY composite is distinguished by widespread, strong southeasterlies across the Gulf of Mexico. The precursor LATE composite reflects the composite presence of a tropical cyclone in the western Caribbean or southern Gulf of Mexico. As with the precursor EARLY composite, the southeasterly flow across the Gulf is much stronger than normal. The composite two days after the onset of the LATE events (not shown) persists in easterly winds across Texas, indicating the importance of slow tropical cyclone movement for extreme rainfall totals. The precursor NONTROP composite is quite different from Fig. 3a, suggesting that a rapid evolution takes place with these non-tropical cyclone events. The precursor wind field, like the other precursors, includes enhanced southeasterly flow across the Gulf of Mexico, and there is a clear pattern of transport from the Caribbean and tropical Atlantic.

Composites two days following event onset (not shown) were used to deduce the typical evolution of events. The 850 hPa winds associated with the EARLY and NONTROP events bear similar patterns to the onset times, but with somewhat weaker wind speeds and less concentrated deceleration over Texas. The two-day LATE composite was dramatically different, with easterly low-level winds across Texas and little or no influx of moisture from the Gulf of Mexico.

At 500 hPa, both the EARLY and LATE composites show the circulation associated with the tropical cyclones in the form of a northerly-southerly wind couplet across south Texas (Fig. 5ab). The strongest part of the circulation is the patch of southerlies over the northwest Gulf of

Mexico, just south of the Texas-Louisiana border. Although the composite jet stream patterns are different, in both cases the jet is well to the north of Texas, with the primary jet in southern Canada or along the US-Canadian border.

We hypothesize that the southerly winds approaching Texas and the lack of a primary jet stream are significantly different from normal. Testing with 1000-member samples shows that the southerly wind at 500 hPa within the box (25N, 30N, 92.5W, 95W) is significantly different from normal at the 99% confidence level for EARLY events and the 95% confidence level for LATE events. However, the mean vector wind at 500 hPa in the area surrounding Texas is not found to be significantly weaker than normal.

In contrast to the tropical cases, the NONTROP 500 hPa composite (Fig. 5c) features a jet stream unusually far south, stretching from central Arizona to northern Oklahoma before heading northeastward toward southern Canada. Texas is in the right entrance region of the jet stream, implying strong upward motion (Bluestein, 1993, pp. 397-401). The strong southwesterly winds in the north-central United States also appear in the 850 hPa composite (Fig. 3a). In the southeastern United States, a large-scale ridge contributes to the strength of the jet stream. The trough-ridge couplet is rather broad, implying that the upper-level pattern would be slow-moving and inhibit the migration of storm systems toward the east.

We hypothesize that the 500 hPa heights are unusually low over the western United States (within the box 35N, 45N, 100W, 117.5W) and unusually high over the eastern United States (within the box 35N, 45N, 72.5W, 90W). Using 1000-member samples, the mean height anomalies in both these regions are found to be significant at the 99% confidence level.

The one unusual feature common to all three 500 hPa composites is southerly 500 hPa flow approaching Texas from the south. This suggests a possible source of tropical midlevel moisture, which would act to increase the precipitation efficiency of any convection.

Summary

The composites show how certain key elements (Doswell et al., 1996) come together over Texas to produce extreme rainfall events:

(a) Unusual amounts of low-level moisture are provided by strong southeasterly winds that carry moisture from the tropical Atlantic and Gulf of Mexico. Near Texas, the winds decelerate, causing the moisture to become deeper. The approaching winds are much stronger than normal and blow from the southeast across the open Gulf rather than from the east.

(b) In the case of tropical cyclones, ascent is provided by the dynamics of the tropical cyclone itself and by upslope winds across Texas on the northern flank of the tropical cyclone. In the other cases, the large-scale upper-level wave and jet streak pattern focuses ascent over Texas.

(c) The tropical cyclones are slow-moving because the jet stream is well to the north at the time the storms make landfall. The other type of event seems to require the presence of a nearby accelerating jet stream, and the systems are quasi-stationary because the jet stream patterns themselves are slow-moving, keeping the ascent focused over Texas.

(d) High precipitation efficiency requires unusually unstable air and mid-level moisture. The composites show that the low and even mid-level air entering Texas originates well to the south, where humidity tends to be higher.

(e) Most key elements of the composites, relating to low-level moisture flux, long-range transport, deep flow from the tropics, and (for NONTROP events) a favorable upper-level wind pattern, are significantly different from climatology at the 95% or greater confidence level.

One should not expect that with these four large-scale elements in place, extreme precipitation is guaranteed. Much depends on the details of air parcel trajectories and the specific geographical relationship among the important weather elements (Roebber and Reuter, 2002). Also not considered in these large-scale composites are the processes by which extreme precipitation can become focused over a several-county area within the larger-scale systems.

METEOROLOGICAL OVERVIEW OF THE 2002 SOUTH-CENTRAL TEXAS FLOOD

The composite analysis suggests several common flow features that are conducive to extreme rainfall in Texas. However, the composite analysis does not indicate how well individual events agree with the composites, nor does it identify the specific dynamical and physical processes that cause the large-scale patterns to form or allow extreme precipitation to develop within these large-scale patterns. In this section, the large-scale patterns associated with the July 2002 South-Central Texas flood are compared to the composites, and the specific dynamical processes that lead to a sustained heavy rainfall event in a particular location are identified.

Comparison with Composites

The 2002 flood was not associated with a tropical cyclone, which would suggest a classification as NONTROP. However, most NONTROP events occur in September or October, so it is not clear *a priori* whether this event will fit the NONTROP blueprint.

The 500 hPa wind patterns associated with the onset of the 2002 flood (Fig. 6a) bear a very strong resemblance to the EARLY composite (Fig. 5a). In agreement with the composite, the 2002 winds have a southerly maximum over the northwest Gulf of Mexico and a northerly wind maximum across southwest Texas. As in the composite, the main jet stream is well to the north, along the US-Canadian border. The absolute wind magnitudes are stronger in Fig. 6a than the composite (Fig. 5a) because of the spatial averaging properties of the compositing process. For example, the compositing process causes a strong jet of uncertain location to appear as a broad, weak, jet. The north-south elongated trough over central Texas, appearing in both the composite and in the 2002 case, seems to be a common characteristic of early-season extreme floods.

The 850 hPa wind pattern (Fig. 6b), after allowing for the weaker composite winds, lies somewhere between the EARLY pattern (Fig. 1a) and the NONTROP pattern (Fig. 3a). The southeasterly concentrated moisture influx (with winds exceeding 12 m s^{-1}) originates in the central Gulf of Mexico, and, like the EARLY composite, the upstream source region for most of this air appears to be the tropical Atlantic. During the next few days (not shown), the southeasterly flow came entirely from the Caribbean and tropical Atlantic. Somewhat less low-level wind deceleration occurs in the 2002 event than in either composite.

The similarity with the EARLY composite is high despite the fact that all events in the EARLY composite were associated with tropical cyclones. This makes the 2002 event highly unusual. The one other early-season non-tropical event (in 1948) closely fit the NONTROP

composite, as did the April 1966 event that was not included in the NONTROP composite. However, in our experience, many other warm-season heavy rain events that do not attain the threshold required for inclusion in this study also resemble the EARLY composite, despite lacking a tropical cyclone. For example, such an event is taking place at the time of this writing (June 8, 2004).

Rainfall History

Analyses of 24-hour accumulated rainfall (Fig. 7) from the Climate Prediction Center of the National Centers for Environmental Prediction (based on preliminary data but consistent with final point totals and radar estimates) show an event remarkable for the persistence of localized heavy rain, day after day. On the scale of the analysis, the first daily accumulated rainfall over 100 mm was for the period ending the morning of June 30. The next five days each brought over 100 mm of rainfall to broad areas north and west of San Antonio (SAT in Fig. 7). During the periods ending July 1 and 2, heavy rain also fell to the south, but otherwise the heaviest precipitation was confined to a three-county area just north of San Antonio. The most extreme period of rainfall had ended by July 6.

Patton and Baker (1977) note the apparent importance of the Balcones Escarpment as a trigger for the development of heavy rain. The Balcones Escarpment passes through San Antonio and extends several hundred km to its west and northeast, providing a rather abrupt increase of about 300 m from the coastal lowlands to the Edwards Plateau. In their study of the August 1978 flood, Caracena and Fritsch (1983) identified the Balcones Escarpment as one of several causes of the localization of the heavy rain.

Visual inspection of radar mosaics from this event indicates that convective cells repeatedly formed and intensified along the Balcones Escarpment. While strong radar echoes were not confined to that area, the repeated occurrence of intense showers led to large rainfall accumulations there. Air flowing over the Balcones Escarpment may reach its level of free convection under the right circumstances, so the mechanical uplift can serve as a convective trigger.

To the extent that the Escarpment served as the trigger of much of the heavy rainfall, the location of heavy rainfall in a situation such as this may be predictable. However, the fact that Caracena and Fritsch (1983) identified several other triggers, such as a cold pool and an elevated dry layer, and were unable to deduce the relative importance of each, suggests that predicting in which events the Escarpment will determine the rainfall location may itself be a challenge.

The Importance of an Upper-Level Disturbance

An EARLY-type extreme rainfall event is favored by strong southeasterly low-level flow and a north-south oriented slow-moving upper-level trough. Strong southeasterly flow is not unusual – the normal winds during that time of year are from the southeast and bring humid air to Texas. For an extreme rainfall event, the southeasterly flow should be configured properly to deliver the high moisture to the latitude and location of Texas. During the 2002 flood, dewpoints in south Texas exceeded 26 °C, an indication of a tropical moisture source or strong moisture fluxes from the nearby sea surface. High dewpoints such as these are common upstream of extreme rainfall events.

To maximize the moisture in Texas, air parcel trajectories should be deflected to the right of their normal course. This way, the most humid air continues north into Texas rather than passing across Central America.

Potential vorticity (PV) thinking is a powerful way of understanding the interactions of weather phenomena in the atmosphere. Introduced by Hoskins et al. (1985), PV thinking relates “anomalies”, regions of anomalously low or high PV compared to their surroundings, to large-scale wind and temperature patterns consistent with atmospheric balance. A positive PV anomaly aloft is associated with a cyclonic (counterclockwise in the Northern Hemisphere) circulation that is strongest at the level of the anomaly and relatively cool temperatures that are coldest directly beneath the anomaly. In the free troposphere, PV can be regarded as being conserved (and therefore evolving solely through advection) except during the formation of precipitation, when PV is destroyed aloft and recreated at low levels. The influence of multiple PV anomalies can be approximated by adding together the anticipated effects of each individual PV anomaly.

In the context of PV thinking, deflecting an airstream to the right can be accomplished by a PV anomaly over the “intended” path of the airstream. Specifically, an upper-level PV anomaly over south Texas would tend to add a southwesterly component to air crossing the Gulf of Mexico from the southeast. At low levels, the influence of the upper-level PV anomaly would be weak. At some appropriate anomaly strength, the deflection of the winds would be ideal to maximize the moisture flux into Texas.

The closed 500 hPa cyclonic circulation that appears in both the composite and the 2002 event can serve this purpose. Such a low center is almost always associated with a positive PV anomaly aloft. Furthermore, the 500 hPa trough or low serves another function that is essential

to extreme rainfall: its locally cold temperatures cause humid low-level air to become increasingly convectively unstable, with the greatest instability beneath the trough. Thus, the PV anomaly associated with the 500 hPa disturbance helps establish a favorable low-level wind pattern and creates the convective instability required to produce high rainfall rates and to confine the event to a particular geographical area. PV anomalies are not necessarily slow-moving, but when a weak one does stall over Texas, all the necessary ingredients are in place for an early-season extreme rainfall event.

Contributory Upper-Level Processes

The upper-level pattern during the latter part of June and the early part of July was conducive to slowly-moving, long-lived upper-tropospheric disturbances. One upper-level cutoff low formed over Georgia on June 21 and drifted westward to the Texas-Arkansas border before being reabsorbed into the westerlies. Another cutoff low first appeared on June 27 just off the California coast and was quasi-stationary for almost a week before drifting east to New Mexico and dissipating. This favorable upper-level flow pattern is the first upper-level contributor to the extreme rainfall event.

To examine the evolution of the event, we begin at 225 hPa, near the tropopause where the PV anomalies were strongest. Figure 8 shows the evolution of PV and wind between June 28 and July 3. On June 28, the high PV in the trough over northern Mexico and southern Texas is rather disorganized, but the strongest PV anomaly has just crossed the coast into the Gulf of Mexico and is triggering deep convection over the southern Gulf (not shown). During the next

few days, the trough drifts northward, and deep convection spreads into Texas. This nearly ideal trough position is the second upper-level contributor to the extreme rainfall event.

Strong divergent flow develops during the next few days, originating over central Texas and curving anticyclonically eastward to the Gulf. This flow is the outflow from the convective updrafts, and the associated destruction of PV leads to a sizable upper-level ridge over the southeastern United States. This ridge helps prevent the trough from advancing eastward and also reinforces the low-level flow of moist air into Texas. The ridge formation is a third contributor to the extreme rainfall event, but one which is present only because extreme rainfall is taking place.

Throughout this period, PV is being destroyed within the convective area, but the trough is reinforced about once every 24 hours by a new piece of high PV being sheared off of the southern edge of the cutoff cyclone near Southern California. The reinforcing PV acts to keep the air columns over Texas unstable and is associated with upward motion as it approaches the Gulf. This supply of additional PV is the fourth upper-level contributor to the extreme rainfall event.

By June 30 and July 1, a band of high PV extends from California to Kansas to Georgia. An extended band of high PV not undergoing strong deformation is barotropically unstable (Dritschel et al., 1991), and indeed this band of PV breaks down into high-amplitude waves by July 2. The band is displaced northward over Utah, southward over New Mexico and the Texas panhandle, northward over Iowa, and southward across the Florida panhandle. This specific configuration is probably due to the structures originally in place: the strong vortex over California and the strong divergent outflow over Oklahoma and Arkansas. As a consequence,

high PV air is advected southward into Texas, further reinforcing the trough over Texas. This barotropic intensification is the fifth upper-level contributor to the extreme rainfall event.

By July 3, much of the high PV associated with the Texas trough has moved southward into northern Mexico and the western Gulf. This movement might have meant the end of the heavy rainfall, but for PV processes taking place lower in the troposphere. Figure 9 shows mid-troposphere PV and winds at two-day intervals. Initially, the PV in the vicinity of Texas is unremarkable. However, the convection generates PV, and in this case the combination of generation and vertical advection produces the largest PV anomalies near the 500 hPa level.

Early in the event, the PV anomalies are advected northward out of the area of heavy rainfall. The PV anomaly in Kansas on July 2 was in central Texas on June 30. However, as the PV at higher levels migrates southward, the wind pattern in the middle troposphere changes over Texas, so that as new PV is generated, it tends to stay in place, helping to form a broad mid-level circulation center across the area. While a mid-level PV anomaly is not effective in increasing the overall instability, it is effective in creating low-level ascent and removing the inhibition to convection within the inflow air approaching from the southeast (Raymond and Jiang, 1990; Trier and Davis, 2002). This quasi-stationary midlevel vortex is the sixth upper-level contributor to the extreme rainfall event.

Summary

The 2002 rainfall event was especially remarkable for its persistence. The key large-scale phenomenon associated with events such as this appears to be a stationary upper-level trough oriented in a north-south direction across Texas. Smaller-scale processes that may have served

to concentrate the heavy rain in a particular location are mostly beyond the scope of this overview, although it appears that the mechanical lifting produced by the Balcones Escarpment contributed to the localization.

We have counted six upper-level events and processes, many of them unusual, that contributed to the duration or intensity of the 2002 flood. This conjunction of favorable events serves as a reminder that favorable large-scale conditions may be necessary for extreme rainfall, but they are by no means sufficient. It also serves as a warning that an extreme event, by its very nature, requires many elements in the atmosphere to come together in just the right way, so that an accurate forecast of an extreme event requires an accurate forecast of all the necessary elements.

PREDICTABILITY OF THE 2002 FLOOD

Introduction

In the preceding section, several large-scale factors were identified that contributed to the extreme nature of the 2002 flood. In addition to the large-scale factors, unconsidered processes operating on the mesoscale and convective scale must also be present, and they all interact to produce the particular event.

Human forecasters who use numerical model output in their forecasts are beginning to have difficulty improving on the quality of the raw numerical forecasts (Charba et al., 2003). As noted before, numerical models have particular difficulty with warm-season convective rainfall, and so do humans. This section considers the ability of a sophisticated numerical model to

accurately predict one day's rainfall from the 2002 flood, and by extension the ability the humans using the model to make accurate predictions.

Uncertainties of a numerical model forecast arise in several ways including inevitable model deficiencies (e.g., finite resolution, inaccurate representation or parameterization of unresolved subgrid-scale processes), finite errors in the initial conditions, and the chaotic nature of the atmosphere (e.g., Lorenz 1969). The sensitivity of a numerical forecast to resolution, parameterizations, and initial conditions is a complex function of the specific meteorological circumstances that depends on the scales of interest and is subject to the underlying dynamics and instability (e.g., Zhang et al. 2003). It is thus of great interest to assess the predictability of weather systems like the 2002 flood under various uncertainties, particularly with respect to the intensity and spatial distribution of the associated precipitation.

Numerical Model and Experiment Design

The Penn State/NCAR Mesoscale Model Version 5 (MM5) is a commonly-used research and operational numerical model with a wide range of available parameterizations (Dudhia 1993). Tests with the model, unless otherwise specified, involve a forecast initialized at 0000 UTC July 1, 2002 (1800 CST June 30) with GCIP datasets derived from the operational NCEP Eta-model analysis and integrated for 36 hours. The forecasted precipitation accumulating between 12 and 36 hours is compared to the analyzed precipitation presented in the preceding section. A variety of control model runs were made, and the specific date and model run chosen for presentation here is one of the best forecasts from the rainfall episode. The forecast covers a period during which the upper-level trough over Texas was being reinforced by additional PV anomalies from

the west. Additional PV from the north was approaching the area due to the onset of barotropic instability.

The Mellor-Yamada boundary-layer (PBL) scheme, Reisner microphysics scheme with graupel and the Grell cumulus parameterization scheme are used for the control experiment (CNTL). The GCIP analysis is also used for the lateral boundary conditions. Aside from the control model run, forecasts are made with two other sets of initial conditions, three other microphysical parameterizations (governing clouds and precipitation), three different cumulus parameterizations (governing convection), three different PBL schemes, two different model grid spacings, and two different forecast lead times. These various experiments and their difference in model configurations with the control experiment are listed in Table 3; brief descriptions and references of various parameterizations can be found in Dudhia et al. (2001).

Baseline model performance is not necessarily optimal. Other studies show that similar forecasts can be improved by appropriate soil moisture initialization (Bernadet et al., 2000) or enhanced atmospheric moisture initialization (Stein et al., 2000). The lack of observations over the Gulf of Mexico makes it difficult for the model to know which air will be most unstable and hence where convection will break out, while the lack of a soil moisture field that includes the effect of the rain that had already fallen eliminates an important feedback mechanism for repeated rainfall events (Xue et al., 2001).

Results

The control model run compares favorably with the observed precipitation distribution at resolvable scales (Fig. 10ab). Because the model grid spacing is 30 km, it would not be expected

to resolve structures with a wavelength smaller than 150-200 km. At the resolution of the model, the forecasted location and intensity of precipitation in the Hill Country area is quite good. Less desirable are two other areas of heavy rainfall, in east Texas and eastern Louisiana, that in reality did not occur.

Changing the initial conditions retains the character of the precipitation but substantially alters the geographical distribution of the precipitation (Fig. 10cd). The NNRP run produces several areas of intense precipitation, including one (too small) near San Antonio. The TOGA run produces even more rainfall, with a tendency for precipitation to be concentrated along the coast. At best, this set of model runs could tell a forecaster that heavy rain is likely somewhere in the southeastern half of Texas. Such a forecast would be of limited value to the public.

In this particular case, the control model run is presumed to use a superior initialization. An alternate way of investigating the sensitivity to initial conditions consists of varying the starting time of the forecast. In this case, moving the start of the forecast forward or backward by 12 hours changes the rainfall forecast significantly (Fig. 11). While some aspects of the simulation are improved by a shorter lead time, others suffer.

The sensitivity of the forecast to various parameterization options is shown in Fig. 12. Changing the microphysics has the smallest effect. All three experimental runs produce a rainfall maximum west of San Antonio. Other rainfall locations are generally consistent from model run to model run, but the specific amounts of rainfall in any given location vary widely.

Changes in the convective parameterization scheme have a large impact on the forecast. Two of the three modified runs fail to produce precipitation in excess of 100 mm. Versions of most of these schemes are in active operational use for numerical weather prediction, and no scheme is considered a priori to be "best". A strong sensitivity to convective schemes, and even

the details within a convective scheme, has been noted in other warm-season studies (Kain and Fritsch, 1992; Gallus, 1999; Cohen, 2002).

The runs with various PBL parameterizations indicate that the model is moderately sensitive to the details of the vertical mixing in this case. Peak precipitation totals easily vary by a factor of two or more. The erroneous heavy precipitation near New Orleans is forecasted more consistently than the correct heavy precipitation near San Antonio.

Several studies have found that improved model resolution leads to more realistic simulation of convective processes (e.g., Belair and Mailhot, 2001), and occasionally the forecasts are improved as well (Bernadet et al., 2000; Zhang et al. 2002). In the present event, increasing the model resolution degrades the forecast (Fig. 13). This result is not too surprising at resolutions (10 km and 30 km) at which a cumulus parameterization is necessary (Molinari and Dudek, 1992; Gallus, 1999), but it is remarkable that explicitly resolving the convection fails to produce a forecast resembling the observed precipitation distribution. Part of this poor performance may be due to lack of convective triggering even at the grid spacing of 3.3km. It may also be due to the potentially detrimental impact of an outer-grid cumulus parameterization on the precipitation simulation in the high-resolution inner nest (Warner and Hsu, 2000; Colle et al., 2003).

Discussion

The numerical experiments presented above suggest that deterministic forecasting of extreme rainfall events at the 1-2 day range will not be possible for the foreseeable future. The wide range of forecasts suggests that some of the suggested non-deterministic uses of mesoscale forecast models may also have difficulty in the context of forecasting extreme rainfall due to

model deficiencies and initial conditions. Moreover, as in Zhang et al. (2003), even if the model's initial conditions are nearly perfect, we have demonstrated significant uncertainties in the rainfall forecast of this event due to the chaotic nature of weather, implying the existence of finite intrinsic limit of predictability (which will be reported elsewhere).

Ensemble forecasts are based on the premise that a set of equally likely (or nearly so) forecasts improve on a deterministic forecast in two ways: by providing information regarding the probability distribution of forecast outcomes, and by providing an ensemble mean forecast which tends to be superior to the forecast of any given ensemble member. The American Meteorological Society (AMS, 2002) has called for increasing use of probabilities in forecasts, for example by forecasting the probability of greater than 25 mm of rain at a given location. Because extreme events are inherently rare, it will be quite some time before modelers and forecasters are able to even measure the skill of probabilistic forecasts of extreme events. If the above set of experimental forecasts is taken as a typical of the expected quality of ensemble forecast guidance, forecasters will have to continue to rely on their own skills and ability to interpret data for quite some time.

CONCLUSION

Extreme rainfall events, defined as 500 mm or more of rain in 7 days or fewer, are in general rare, although they are more common in Texas than in most other parts of the United States. Most such events occur in the summer or early fall.

Through a composite analysis, three distinct large-scale weather patterns were found to be associated with extreme rainfall events. The EARLY composite consists of events in June, July,

and August. Most such events are associated with landfalling or developing tropical storms. The common characteristic of EARLY events is a small-scale 500 hPa trough oriented north-south across Texas, with the jet stream well to the north. The LATE composite consists of September tropical cyclone events. The jet stream is well to the north in these events too, allowing the hurricane to stall and produce sustained easterly upslope flow across Texas. The NONTROP cases occur almost entirely in September and October. In contrast to the other two cases, the jet stream is located unusually far south, with Texas beneath the right entrance region of a jet streak. This upper-level configuration ensures widespread ascent across Texas. All three patterns feature strong low-level flow from the southeast, usually originating over the Caribbean Sea or the tropical Atlantic Ocean. The enhanced low-level inflow was statistically significant, as were the 500 hPa southerlies for EARLY and LATE events and the 500 hPa trough-ridge pattern in the NONTROP cases.

The 2002 South-Central Texas Flood was an EARLY event, both according to the calendar and according to agreement with the composite. The event was remarkable for its duration, as heavy rainfall was regenerated day after day along the Balcones Escarpment near San Antonio. An unlikely combination of several events was found to maintain the upper-level support for the extreme rainfall for a week.

Numerical simulations of the 2002 flood were occasionally successful, providing hope that such events may some day be forecastable well in advance. However, the wide range of forecast outcomes with equally valid model configurations suggests that such a day is well into the future. The model forecasts were particularly sensitive to initial conditions, cumulus parameterizations, and model resolution. The poor performance by many of the numerical model runs suggests that humans still have considerable room to improve upon model output when making forecasts of

extreme weather events, and that such forecasts should be probabilistic rather than deterministic in character.

Acknowledgments: This work was partially supported by the National Science Foundation under grants ATM-0089906 and ATM-0205599, by the National Oceanographic and Atmospheric Administration under cooperative agreement NA17WA1011, and by the Office of Naval Research under grant N000140410471.

REFERENCES

- American Meteorological Society (2002) Enhancing weather information with probability forecasts. *Bulletin of the American Meteorological Society*, Vol. 83, 450-452.
- Asquith, W. H. (1998) *Depth-Duration Frequency of Precipitation in Texas*. Austin, TX: U.S. Geological Survey Water-Resources Investigations Report 98-4044.
- Belair, S. and Mailhot, J. (2001) Impact of horizontal resolution on the numerical simulation of a midlatitude squall line: Implicit versus explicit condensation. *Monthly Weather Review*, Vol. 129, 2362-2376.
- Bernadet, L. R., Grasso, L. D., Nachamkin, J. E., Finley, C. A. and Cotton, W. R. (2000) Simulating convective events using a high-resolution mesoscale model. *Journal of Geophysical Research – Atmospheres*, Vol. 105, 14963-14982.
- Bluestein, H. B. (1993) *Synoptic-Dynamic Meteorology in Midlatitudes, Volume II: Observations and Theory of Weather Systems*. New York: Oxford University Press.
- Bosart, L. F. (1984) The Texas coastal rainstorm of 17-21 September 1979: An example of synoptic-mesoscale interaction. *Monthly Weather Review*, Vol. 112, 1108-1133.

Bosart, L. F., Lai, C.-C. and Weisman, R. A. (1992) A case study of heavy rainfall associated with weak cyclogenesis in the northwest Gulf of Mexico. *Monthly Weather Review*, Vol. 120, 2469-2500.

Caracena, F. and Fritsch, J. M. (1983) Focusing mechanisms in the Texas Hill Country flash floods of 1978. *Monthly Weather Review*, Vol. 111, 2319-2332.

Charba, J. P., Reynolds, D. W., McDonald, B. E. and Carter, G. M. (2003) Comparative verification of recent quantitative precipitation forecasts in the National Weather Service: A simple approach for scoring forecast accuracy. *Weather and Forecasting*, Vol. 18, 161-183.

Cohen, C. (2002) A comparison of cumulus parameterizations in idealized sea-breeze simulations. *Monthly Weather Review*, Vol. 130, 2554-2571.

Colle, B. A., Olson, J. B. and Tongue, J. S. (2003) Multiseason verification of the MM5. Part II: Evaluation of high-resolution precipitation forecasts over the northeastern United States. *Weather and Forecasting*, Vol. 18, 458-480.

Doswell, C. A. III, Brooks, H. E. and Maddox, R. A. (1996) Flash flood forecasting: An ingredients-based methodology. *Weather and Forecasting*, Vol. 11, 560-581.

Dritschel, D. G., Haynes, P. H., Juckes, M. N. and Shepherd, T. G. (1991) The stability of a 2-dimensional vorticity filament under uniform strain. *Journal of Fluid Mechanics*, Vol. 328, 129-160.

Dudhia, J. (1993) A nonhydrostatic version of the Penn State/NCAR Mesoscale Model: Validation tests and simulation of an Atlantic cyclone and cold front. *Monthly Weather Review*, Vol. 121, 1493-1513.

Dudhia, J. and Coauthors (2001) *PSU/NCAR Mesoscale Modeling System Tutorial Class Notes and User's Guide*. Boulder, CO: National Center for Atmospheric Research (available online at <http://www.mmm.ucar.edu/mm5/doc.html>)

Gallus, W. A. Jr. (1999) Eta simulations of three extreme precipitation events: Sensitivity to resolution and convective parameterization. *Weather and Forecasting*, Vol. 14, 405-426.

Gallus, W. A. Jr. (2002) Impact of verification grid-box size on warm-season QPF skill measures. *Weather and Forecasting*, Vol. 17, 1296-1302.

Grice, G. K. and Maddox, R. A. (1982) *Synoptic Aspects of Heavy Rain Events in South Texas Associated with the Westerlies*. Fort Worth, TX: NOAA Technical Memorandum NWS SR-106. Available from NTIS PB84115096.

Hill, J. D. (1980) An apparent new record for extreme rainfall. *Weatherwise*, Vol. 33, 157-161.

Hirschboeck, K. K. (1987) Catastrophic flooding and atmospheric circulation anomalies. In *Catastrophic Flooding*, Mayer, L. and Nash, D., eds. London, UK: George Allen & Unwin, pp. 23-56.

Hoskins, B. J., McIntyre, M. E. and Robertson, A. W. (1985) On the use and significance of isentropic potential vorticity maps. *Quarterly Journal of the Royal Meteorological Society*, Vol. 111, 877-946.

Igau, R. C. and Nielsen-Gammon, J. W. (1998) Low-level jet development during a numerically-simulated return flow event. *Monthly Weather Review*, Vol. 126, 2972-2990.

Kain, J. S. and Fritsch, J. M. (1992) The role of the convective “trigger function” in numerical forecasts of mesoscale convective systems. *Meteorology and Atmospheric Physics*, Vol. 49, 93-106.

Kalnay, E. and Coauthors (1996) The NCEP/NCAR 40-Year Reanalysis Project. *Bulletin of the American Meteorological Society*, Vol. 77, 437-471.

Konrad, C. E. II (2001) The most extreme precipitation events over the eastern United States from 1950-1996: Considerations of scale. *Journal of Hydrometeorology*, Vol. 2, 309-325.

Kunkel, K. E., Andsager, K. and Easterling, D. R. (1999) Long-term trends in extreme precipitation events over the conterminous United States and Canada. *Journal of Climate*, Vol. 12, 2515-2527.

Lanning-Rush, J., Asquith, W. H. and Slade, R. M. Jr. (1998) *Extreme Precipitation Depths for Texas, Excluding the Trans-Pecos Region*. Austin, TX: U.S. Geological Survey Water-Resources Investigations Report 98-4099.

Lorenz, E. N. (1969) The predictability of a flow which possesses many scales of motion. *Tellus*, Vol. 21, 289-307.

Maddox, R. A., Chappell, C. F. and Hoxit, L. R. (1979) Synoptic and meso-alpha aspects of flash flood events. *Bulletin of the American Meteorological Society*, Vol. 60, 115-123.

Molinari, J. and Dudek, M. (1992) Parameterization of convective precipitation in mesoscale models: A critical review. *Monthly Weather Review*, Vol. 120, 326-344.

Nicolini, M., Waldron, K. M. and Paegle, J. (1993) Diurnal oscillations of low-level jets, vertical motion and precipitation: A model case study. *Monthly Weather Review*, 121, 2588-2610.

NOAA (2001) *Tropical Storm Allison Heavy Rains and Floods Texas and Louisiana June 2001*. U.S. Department of Commerce, NWS Service Assessment.

Olson, D. A., Junker, N. W. and Korty, B. (1995) Evaluation of 33 years of quantitative precipitation forecasting. *Weather and Forecasting*, Vol. 10, 498-511.

Patton, P. C. and Baker, V. R. (1977) Geomorphic response of central Texas stream channels to catastrophic rainfall and runoff. In *Geomorphology of Arid Regions*, Doehring, D. O., ed. London, UK: George Allen & Unwin, 189-217.

Petroski, T. J. (2000) *Numerical Simulation of the 16-19 October 1994 Southeast Texas Heavy Rain Event: Precipitation Results and Diagnosis of the Lifting Mechanism*. M.S. Thesis, College Station, TX: Texas A&M University.

Raymond, D. J. and Jiang, H. (1990) A theory for long-lived mesoscale convective systems. *Journal of the Atmospheric Sciences*, Vol. 47, 3067-3077.

Roebber, P. J. and Reuter, G. W. (2002) The sensitivity of precipitation to circulation details. Part II: Mesoscale modeling. *Monthly Weather Review*, Vol. 130, 3-23.

Schultz, D. M., Cortinas, J. V. Jr. and Doswell, C. A. III (2002) Comments on "An operational ingredients-based methodology for forecasting midlatitude winter season precipitation". *Weather and Forecasting*, Vol. 17, 160-167.

Scott, R. K. (2001) *The South Central Texas Heavy Rain Event of October 1998: An MM5 Simulation and Diagnosis of Convective Initiation*. M.S. Thesis, College Station, TX: Texas A&M University.

Smith, J. A., Baeck, L., Morrison, J. E. and Sturdevant-Rees, P. (2000) Catastrophic rainfall and flooding in Texas. *Journal of Hydrometeorology*, Vol. 1, 5-25.

Stein, J., Richard, E., Lafore, J. P., Pinty, J. P., Asencio, N. and Cosma, S. (2000) High-resolution non-hydrostatic simulations of flash-flood episodes with grid-nesting and ice-phase parameterizations. *Meteorology and Atmospheric Physics*, Vol. 72, 203-221.

Stensrud, D. J. and Fritsch, J. M. (1994) Mesoscale convective systems in weakly forced large-scale environments. Part II: Generation of a mesoscale initial condition. *Monthly Weather Review*, Vol. 122, 2068-2083.

Trier, S. B. and Davis, C. A. (2002) Influence of balanced motions on heavy precipitation with a long-lived convectively generated vortex. *Monthly Weather Review*, Vol. 130, 877-899.

Wang, W. and Seaman, N. L. (1997) A comparison study of convective parameterization schemes in a mesoscale model. *Monthly Weather Review*, Vol. 125, 253-278.

Warner, T. T. and Hsu, H.-M. (2000) Nested-model simulation of moist convection: The impact of coarse-grid parameterized convection on fine-grid resolved convection. *Monthly Weather Review*, Vol. 128, 2211-2231.

Xue, Y., Zeng, F. J., Mitchell, K. E., Janjic, Z. and Rogers, E. (2001) The impact of land surface processes on simulations of the U.S. hydrological cycle: A case study of the 1993 flood using the SSiB land surface model in the NCEP Eta regional model. *Monthly Weather Review*, Vol. 129, 2833-2860.

Zhang, F., Snyder, C. and Rotunno, R. (2002) Mesoscale predictability of the 'surprise' snowstorm of 24-25 January 2000. *Monthly Weather Review*, Vol. 130, 1617-1632.

Zhang, F., Snyder, C. and Rotunno, R. (2003) Effects of moist convection on mesoscale predictability. *Journal of the Atmospheric Sciences*, Vol. 60, 1173-1185.

Table 1. Extreme Rainfall Events in Texas, 1948-2001^a

Event dates (onset date for composite in parentheses)	County or location	Maximum amount (mm) /duration ^b	Event classification	Associated tropical cyclone ^c
23-24 June 1948 (24)	Val Verde	600+ /24 hrs	NONTROP	
12-16 Sept 1951 (13)	Coastal plain	530 /5 days	NONTROP	
9-11 Sept 1952 (10)	Blanco	526 /24 hrs	NONTROP	
24-29 June 1954 (25)	Crockett	860 /6 days	EARLY	Hurr. Alice
23-25 Sept 1955 (24)	Val Verde	610 /3 days	NONTROP	
24-26 June 1960 (25)	Port Lavaca	760+ /3 days	EARLY	Unnamed T.S.
17-19 Sept 1963 (18)	Newton	595 /3 days	LATE	Hurr. Cindy
22-25 April 1966	Gladewater	578 /2.5 days	^d	
19-25 Sept 1967 (20)	Nueces River	860 /7 days	LATE	Hurr. Beulah
7-13 Sept 1971 (8)	Bee	660 /7 days	LATE	Hurr. Fern
1-4 Aug 1978 (2)	Bandera	1220+ /3 days	EARLY	T.S. Amelia
24-28 July 1979 (25)	Brazoria	1090 /24 hrs ^e	EARLY	T.S. Claudette
17-21 Sept 1979 (18)	Brazoria	680 /5 days	NONTROP	
5-10 Sept 1980 (7)	Kimble	630 /2 days?	LATE	T.S. Danielle
16-19 Sept 1984 (17)	Cameron	510+ /4 days	NONTROP	
19 Oct 1984 (19)	San Patricio	630 /3.5 hrs	NONTROP	
11-12 Nov 1984	Colorado	530 /2 days	^d	
15-19 Oct 1994 ^f (16)	Liberty	775 /3 days	NONTROP	

17-19 Oct 1998 ^g (18)	Comal	760 /2 days	NONTROP	
4-10 June 2001 ^h (10)	Harris	684 /10 hrs	EARLY	T.S. Allison
30 Jun-6 Jul 2002	Bexar	857 /7 days	^d	

^aSource for 1948-1994 events: Lanning-Rush et al. (1998), except where noted

^bThreshold for inclusion: at least 500 mm over at most 7 days

^cHurr. = Hurricane; T.S. = Tropical Storm

^dNot included in classification. See text for explanation.

^eHill (1980) ^fPetroski (2000) ^gScott (2001) ^hNOAA (2001)

Table 2. Tests of the significance of mean 850 hPa winds at 90W

Composite	N-S envelope for averaging	Direction of wind toward Texas (degrees)	Significance of strong wind speed	Likelihood of favorable wind direction
EARLY	17.5N-25N	105-140	97%	1%
LATE	20N-30N	120-155	98%	16%
NONTROP	20N-27.5N	115-150	99%	3%

Table 3. Tests of the sensitivity of simulated precipitation to aspects of the numerical simulations

Model run	Difference from CNTL	Model run	Difference from CNTL
NNRP	Initialized with NNRP analyses	BM	Betts-Miller cumulus scheme
TOGA	Initialized with TOGA analyses	KA	Kuo-Anthes cumulus scheme
24h	Initialized at 1200 UTC 1 July	MRF	MRF PBL scheme
48h	Initialized at 1200 UTC 30 June	GS	Gayno-Seaman PBL scheme
GD	Goddard microphysics scheme	BT	Burk-Thompson PBL scheme
SI	Simple ice microphysics scheme	10km	10 km horizontal grid spacing
Sh	Schultz microphysics scheme	3.3km	3.3 km horizontal grid spacing
KF	Kain-Fritsch cumulus scheme		

FIGURE CAPTIONS

Fig. 1. Composite 850 hPa vector winds and wind speeds (shading, m s^{-1}), (a) EARLY event onset days; (b) reference normal composite (one year after onset days).

Fig. 2. Composite 850 hPa vector winds and wind speeds (shading, m s^{-1}), (a) LATE event onset days; (b) reference normal composite (one year after onset days).

Fig. 3. Composite 850 hPa vector winds and wind speeds (shading, m s^{-1}), (a) NONTROP event onset days; (b) reference normal composite (one year after onset days).

Fig. 4. Composite 850 hPa vector winds and wind speeds (shading, m s^{-1}), two days prior to onset of (a) EARLY events; (b) LATE events; (c) NONTROP events.

Fig. 5. Composite 500 hPa vector winds and wind speeds (shading, m s^{-1}) at onset of (a) EARLY events; (b) LATE events; (c) NONTROP events.

Fig. 6. Vector winds and wind speeds (shading, m s^{-1}) at onset (0000 UTC 30 June 2002) of South-Central Texas flood, (a) 500 hPa; (b) 850 hPa.

Fig. 7. Analyzed accumulated precipitation during 2002 South-Central Texas flood, for successive 24-hour periods beginning and ending at 1200 UTC. Also shown is the storm total for the 8-day period. The location of San Antonio is indicated by "SAT". Unshaded contours are at 10 mm, 50 mm, 75 mm, 125 mm, 200 mm, 300 mm, and 500 mm.

Fig. 8. Upper-tropospheric potential vorticity (200-250 hPa layer mean) and wind vectors (225 hPa level) at 1200 UTC on the indicated dates. A vector equal in length to the plotted vector spacing corresponds to a wind speed of 9 m s^{-1} .

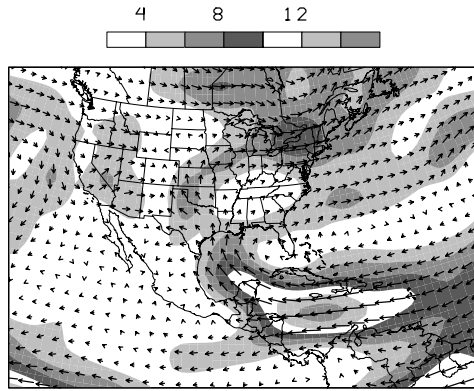
Fig. 9. Middle-tropospheric potential vorticity (400-600 hPa layer mean) and wind vectors (500 hPa level), plotted as in Fig. 8.

Fig. 10. 24-hour accumulated precipitation (every 20 mm) for period ending 1200 UTC 2 July 2002, (a) CNTL simulation; (b) observed; (c) NNRP simulation; (d) TOGA simulation. Dot indicates location of San Antonio.

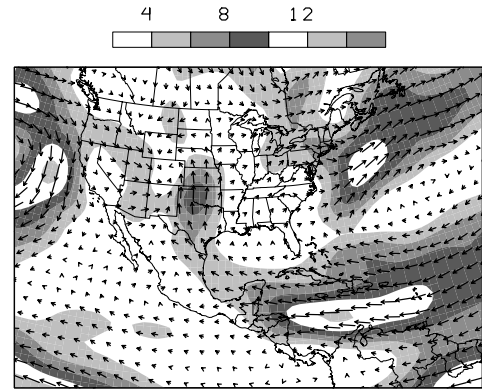
Fig. 11. 24-hour accumulated precipitation, as in Fig. 10, but for simulations initialized at (a) 1200 UTC 1 July; (b) 1200 UTC 30 June.

Fig. 12. 24-hour accumulated precipitation, as in Fig. 10, but for simulations involving the indicated changes in model parameterizations.

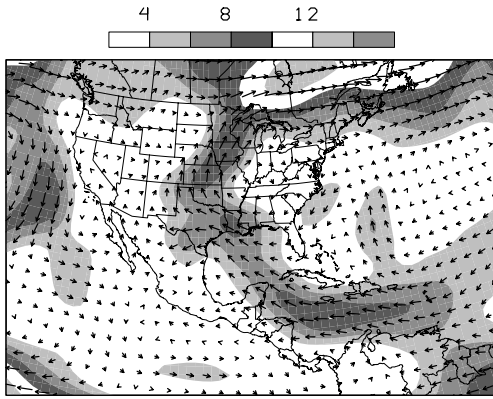
Fig. 13. 24-hour accumulated precipitation, as in Fig. 10, but for simulations run with grid spacings of (a) 10 km; (b) 3.3 km.



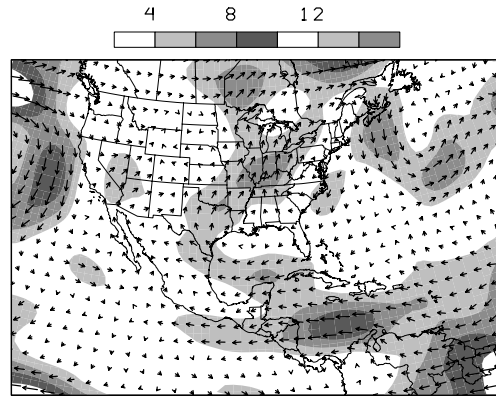
(a) 850 hPa EARLY



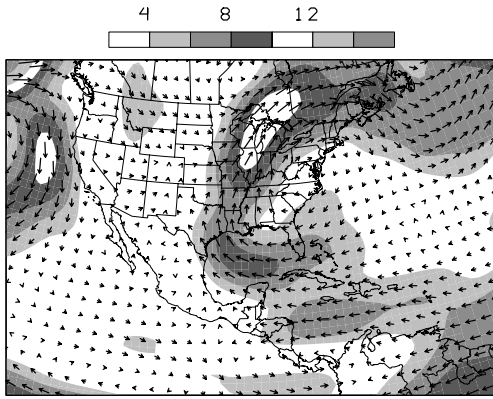
(b) 850 hPa EARLY +1yr



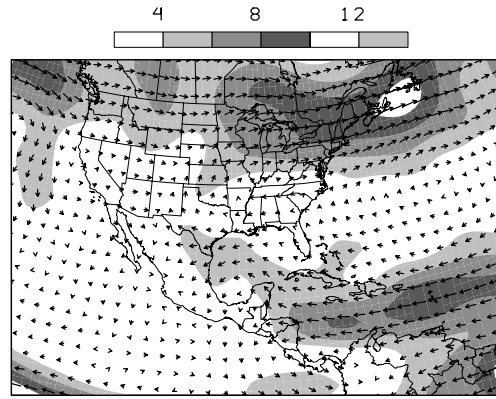
(a) 850 hPa LATE



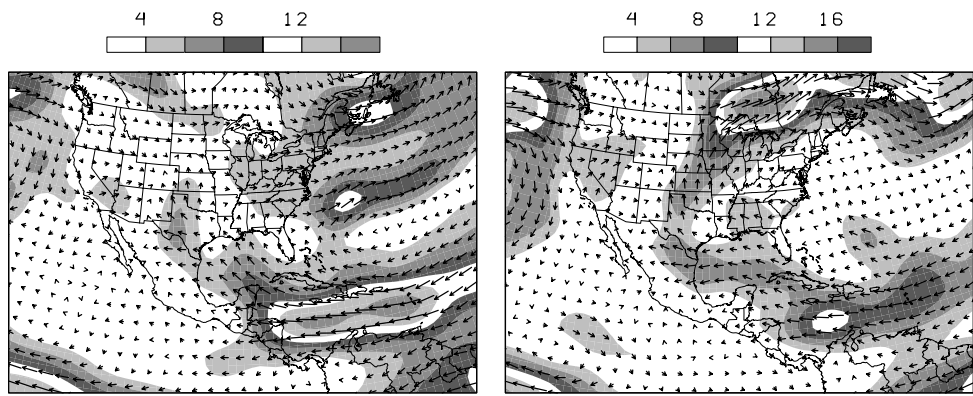
(b) 850 hPa LATE +1yr



(a) 850 hPa NONTROP

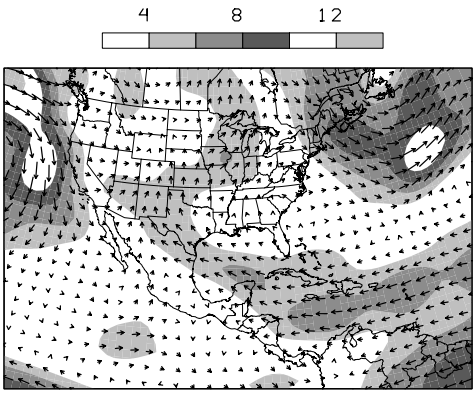


(b) 850 hPa NONTROP +1yr

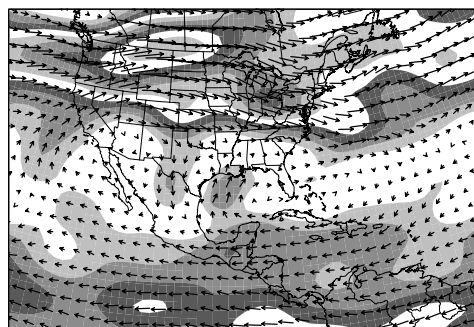


(a) 850 hPa EARLY -2dy

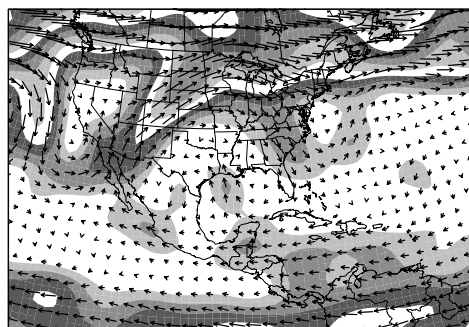
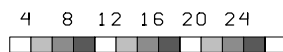
(b) 850 hPa LATE -2dy



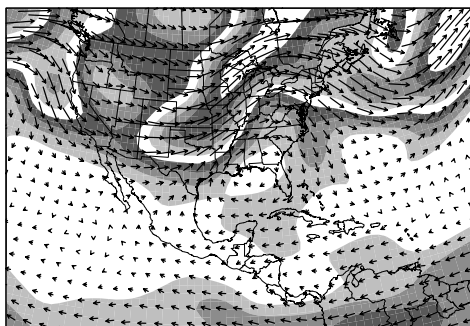
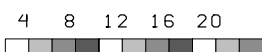
(c) 850 hPa NONTROP -2dy



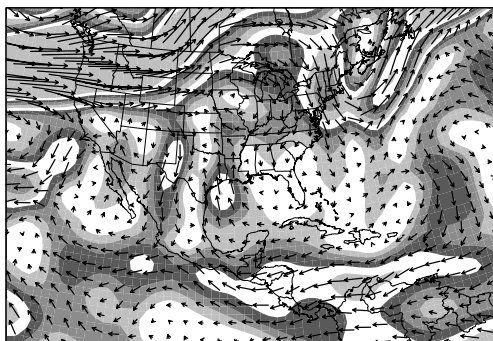
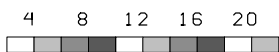
(a) 500 hPa EARLY



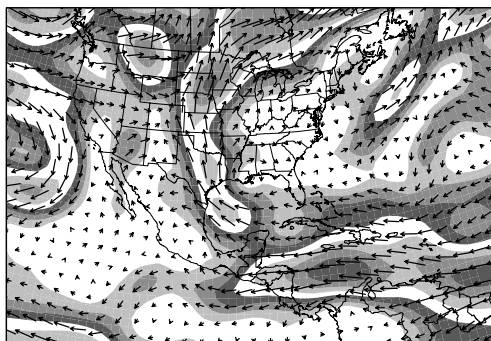
(b) 500 hPa LATE



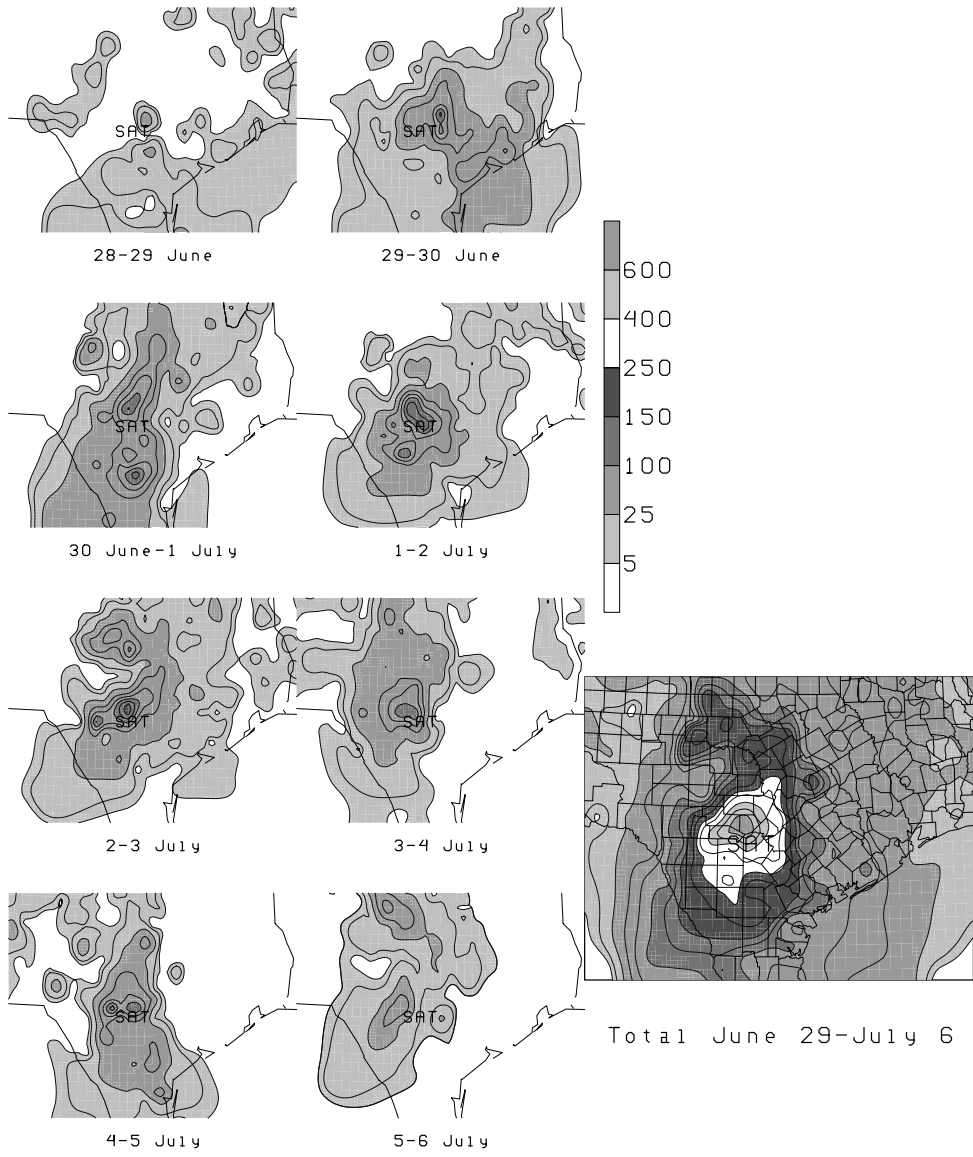
(c) 500 hPa NONTROP



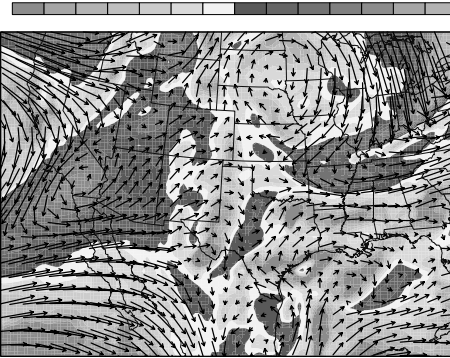
(a) 500 hPa 30 Jun 2002



(b) 850 hPa 30 Jun 2002

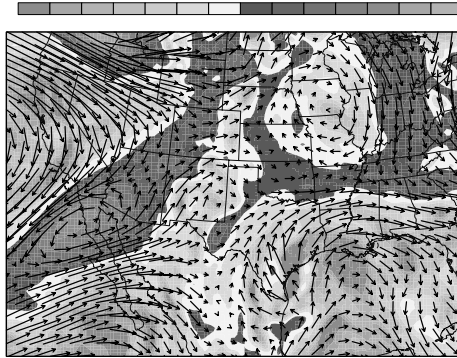


0. 10 0. 28 0. 56 1. 10 2. 30 4. 60 9. 20



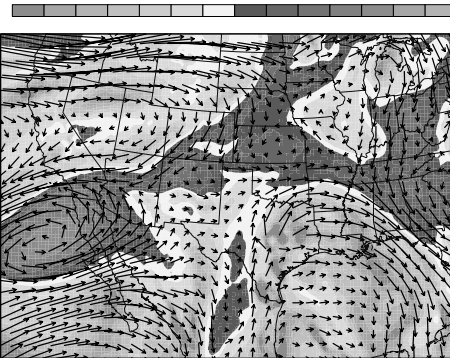
(a) 28 Jun 2002 Uppertrop PV

0. 10 0. 28 0. 56 1. 10 2. 30 4. 60 9. 20



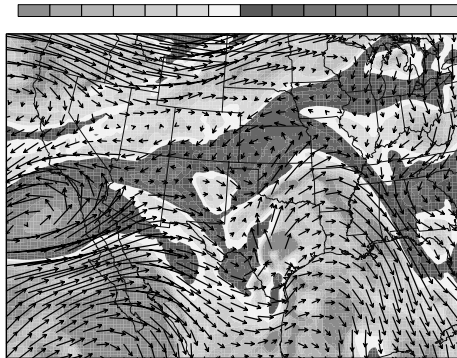
(b) 29 Jun 2002 Uppertrop PV

0. 10 0. 28 0. 56 1. 10 2. 30 4. 60 9. 20



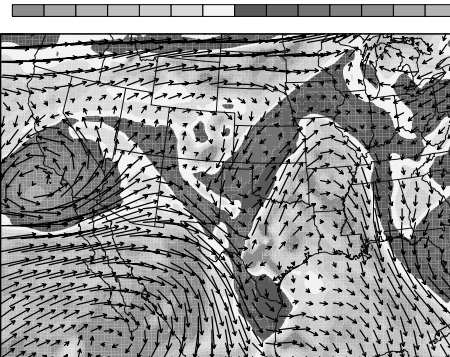
(c) 30 Jun 2002 Uppertrop PV

0. 10 0. 28 0. 56 1. 10 2. 30 4. 60 9. 20



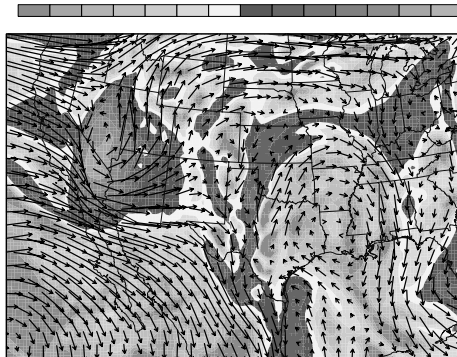
(d) 01 Jul 2002 Uppertrop PV

0. 10 0. 28 0. 56 1. 10 2. 30 4. 60 9. 20



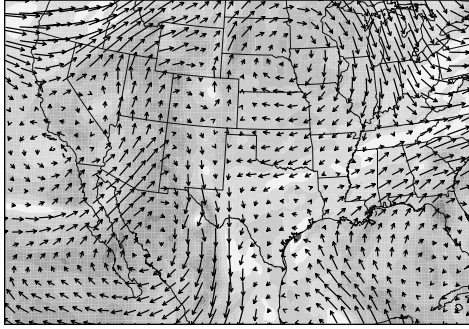
(e) 02 Jul 2002 Uppertrop PV

0. 10 0. 28 0. 56 1. 10 2. 30 4. 60 9. 20



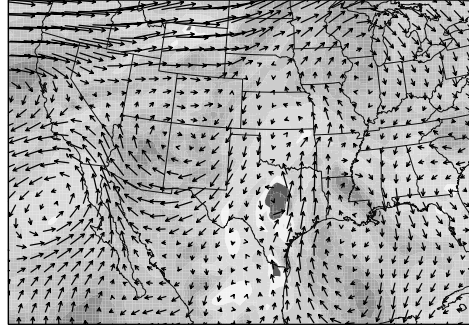
(f) 03 Jul 2002 Uppertrop PV

0.10 0.28 0.56 1.10 2.30 4.60



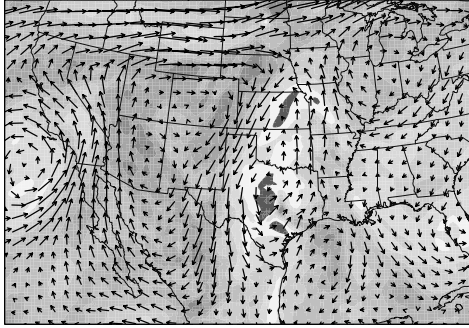
(a) 28 Jun 2002 Midtrop PV

0.10 0.28 0.56 1.10 2.30 4.60



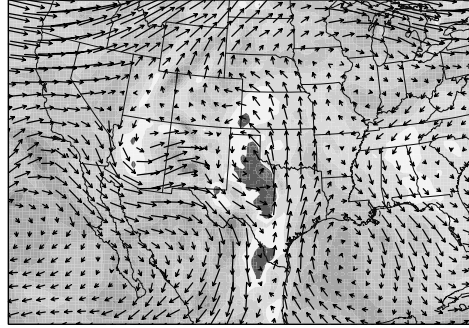
(b) 30 Jun 2002 Midtrop PV

0.10 0.28 0.56 1.10 2.30 4.60



(c) 02 Jul 2002 Midtrop PV

0.10 0.28 0.56 1.10 2.30 4.60



(d) 04 Jul 2002 Midtrop PV

